Clim Dyn (2018) 50:4335–4346
DOI 10.1007/s00382-017-3878-4

Covariability of Central America/Mexico winter precipitation and tropical sea surface temperatures

Yutong Pan[1,3,5] · Ning Zeng[1] · Annarita Mariotti[2] · Hui Wang[3] · Arun Kumar[3] · René Lobato Sánchez[4] · Bhaskar Jha[3,5]

Received: 21 August 2016 / Accepted: 1 June 2017 / Published online: 30 August 2017

Abstract In this study, the relationships between Central America/Mexico (CAM) winter precipitation and tropical Pacific/Atlantic sea surface temperatures (SSTs) are examined based on 68-year (1948–2015) observations and 59-year (1957–2015) atmospheric model simulations forced by observed SSTs. The covariability of the winter precipitation and SSTs is quantified using the singular value decomposition (SVD) method with observational data. The first SVD mode relates out-of-phase precipitation anomalies in northern Mexico and Central America to the tropical Pacific El Niño/La Niña SST variation. The second mode links a decreasing trend in the precipitation over Central America to the warming of SSTs in the tropical Atlantic, as well as in the tropical western Pacific and the tropical Indian Ocean. The first mode represents 67% of the covariance between the two fields, indicating a strong association between CAM winter precipitation and El Niño/La Niña, whereas the second mode represents 20% of the covariance. The two modes account for 32% of CAM winter precipitation variance, of which, 17% is related to the El Niño/La Niña SST and 15% is related to the SST warming trend. The atmospheric circulation patterns, including 500-hPa height and low-level winds obtained by linear regressions against the SVD SST time series, are dynamically consistent with the precipitation anomaly patterns. The model simulations driven by the observed SSTs suggest that these precipitation anomalies are likely a response to tropical SST forcing. It is also shown that there is significant potential predictability of CAM winter precipitation given tropical SST information.

Keywords Precipitation · Sea surface temperature · Central America · Mexico

✉ Yutong Pan
ytpan@umd.edu

[1] Department of Atmospheric and Oceanic Science, University of Maryland, College Park, MD, USA

[2] NOAA/OAR/Climate Program Office, Silver Spring, MD, USA

[3] NOAA/NWS/NCEP/Climate Prediction Center, College Park, MD, USA

[4] The Mexican Institute of Water Technology, Jiutepec, Morelos, Mexico

[5] Innovim, Greenbelt, MD, USA

1 Introduction

Since the beginning of the twenty-first century, widespread droughts have been striking Central America, leading to devastating social and economic impacts. According to a report from the United Nations (OCHA 2014), about two and a half million people in Central America are at the risk of food insecurity. Further to the north, a prolonged drought has also been afflicting Mexico, which reduced Mexico's agricultural production by 40% (Rodriguez 2012). The threat for the drought state in Central America/Mexico (CAM) immediately raises a question as to what the contributing factors are.

Sea surface temperatures (SSTs) in the adjacent oceans have been identified as an important factor modulating the precipitation in CAM (e.g., Cavazos and Hastenrath 1990; Enfield 1996; Enfield and Alfaro 1999; Pavia et al. 2006; Karnauskas and Busalacchi 2009; Mendez and Magana 2010; Bhattacharya and Chiang 2014), including El Niño–Southern Oscillation (ENSO) and tropical Atlantic SST. The former is a major source of interannual variability of CAM precipitation (e.g., Giannini et al. 2000), whereas the latter is a proxy of global warming used for future climate projection for CAM (e.g., Fuentes-Franco et al. 2015).

The associations between CAM precipitation and Pacific/Atlantic SSTs have been examined in many previous studies. It is well recognized that winter precipitation in most of Mexico tends to be above-normal (below-normal) during El Niño (La Niña) years and precipitation anomalies in Central America tend to be opposite (e.g., Cavazos and Hastenrath 1990; Magana et al. 2003; Seager et la. 2009). It is also found that there is a strong association between CAM precipitation and Atlantic SST (e.g., Enfield 1996; Enfield and Alfaro 1999; Taylor et al. 2002). From a historical perspective, however, the relative importance of the SSTs in the two tropical ocean sectors, and their contributions to the CAM precipitation variability have not been quantified. A better understanding of this issue is essential for improving seasonal prediction of CAM precipitation.

The present study is aimed at quantifying the relationships between wintertime CAM precipitation and tropical SSTs based on historical data. The primary foci are (a) to identify the winter precipitation patterns in CAM that tend to occur concurrently with the leading modes of tropical SST variability, (b) to determine the relative importance of tropical Pacific and Atlantic SSTs to the CAM precipitation, (c) to verify whether the observed relationships result from an atmospheric response to tropical SST forcing with atmospheric model simulations, and (d) to assess the potential predictability of CAM winter precipitation knowing tropical SST distribution.

2 Data and methods

The data used in this study consist of precipitation, SST, atmospheric wind, and geopotential height fields. For the observational analysis, the precipitation data are taken from the National Oceanic and Atmospheric Administration (NOAA) Precipitation Reconstruction over Land (PREC/L) dataset (Chen et al. 2002) on a $1^\circ \times 1^\circ$ (latitude $\times$ longitude) grid. The SSTs are the NOAA Extended Reconstructed SST (ERSST) version 3b (Smith et al. 2008) on a $2^\circ \times 2^\circ$ grid. The atmospheric wind and height fields are from the National Centers for Environmental Prediction–National Center for Atmospheric Research (NCEP–NCAR) Reanalysis product (Kalnay et al. 1996) with a $2.5^\circ \times 2.5^\circ$ resolution.

All the observational data are monthly means over a 68-year period from 1948 to 2015. Wang and Fu (2000) demonstrated that a typical ENSO-forced circulation pattern emerges in January and persists through March. Therefore, winter seasonal means in this study are the averages of the monthly mean data of January, February, and March (JFM). An anomaly is defined as the deviation of a seasonal mean from its 68-year climatology.

The relationships between CAM winter precipitation and tropical Pacific/Atlantic SSTs are examined by using the singular value decomposition (SVD) method (Bretherton et al. 1992). This statistical approach can pick out pairs of spatial patterns of precipitation and SST with maximum temporal covariance between the two fields (e.g., Ting and Wang 1997; Wang and Ting 2000; Wang et al. 2010, 2012; Wang and Kumar 2015). Correlation and linear regression against the SVD time series of precipitation and/or SST are used to document and composite the associated atmospheric circulations. The statistical significance of the correlation coefficients is estimated by the two-tailed t-test (Snedecor and Cochran 1989).

The SVD analysis identifies empirical linkages between precipitation and SST, but it does not infer any causal relationships between the two fields. Whether the precipitation–SST linkages obtained based on observational data are atmospheric responses to SST is further verified with Atmospheric Model Intercomparison Project (AMIP) simulations in which SST is prescribed as a forcing. The model used is the NCEP Global Forecast System (GFS), an atmospheric component of the NCEP Climate Forecast System (CFS) version 2 (Saha et al. 2014). The model has a horizontal resolution of T126 (~105 km) and 64 vertical layers. The model was forced by the observed time-varying global monthly SSTs with the Hadley Centre Sea Ice and SST (HadISST) dataset (Rayner et al. 2003) for 1957–2008 and the NOAA Optimum Interpolation SST (OISST) v2 (Reynolds et al. 2002) afterwards. During model integration, observed monthly mean SSTs are linearly interpolated to daily values. It was also forced by the observed time-varying sea ice and greenhouse gas concentrations. The model simulations consist of 18 realizations, each starting from a different initial condition on 1 January 1957 and integrated from 1957 to 2015. Our analysis focuses on the 18-member ensemble averages of the JFM data over the 1957–2015 period.

3 Results

3.1 Long-term mean and variability of winter precipitation

The observed long-term mean winter precipitation shown in Fig. 1a is characterized by abundant precipitation (>2 mm day^{-1}) over Central America. In contrast, Mexico is dry in winter with mean precipitation less than 1 mm day^{-1} across most of the country. The variability of winter precipitation (Fig. 1b), which is quantified by the standard deviation of JFM seasonal mean precipitation, displays a spatial distribution with strong variability in Central America and weak variability to the north. Figure 1 indicates that large interannual precipitation anomalies are generally associated with large mean precipitation. This is consistent with the fact that

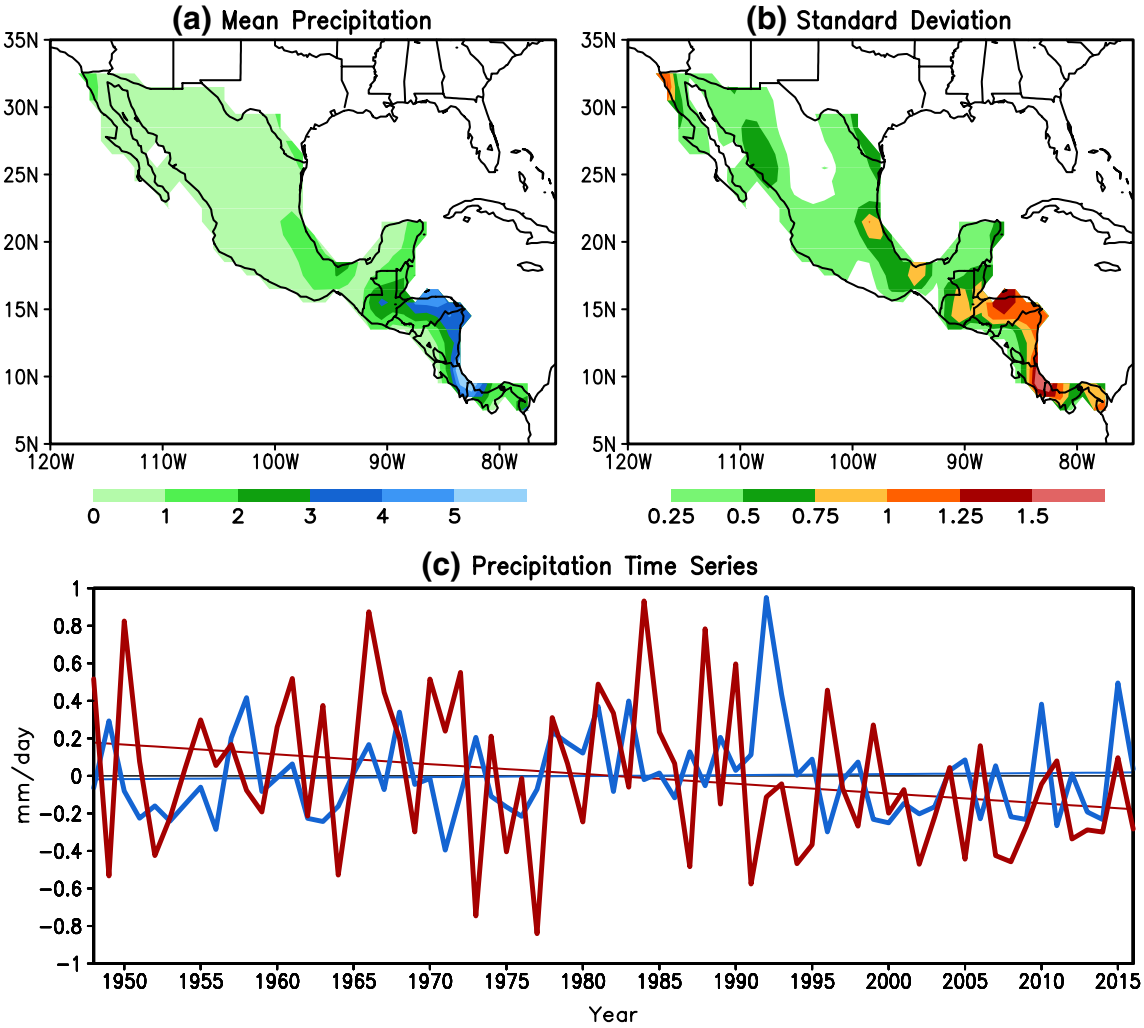

Fig. 1 **a** Climatological seasonal mean (mm day^{-1}) and **b** standard deviation (mm day^{-1}) of winter (JFM) precipitation in Central America and Mexico based on 1948–2015 observations, and **c** time series of precipitation anomalies (mm day^{-1}) averaged over Central America south of 17°N (*thick red line*) and Mexico north of 17°N (*thick blue line*). The *thin red* and *blue lines* in **c** are the corresponding linear trends

the variability of precipitation is characterized by a gamma distribution for which mean and standard distribution are proportional (e.g., Peng and Kumar 2005; Chen and Kumar 2016).

Figure 1c shows the time series of winter precipitation anomalies averaged over Central America (south of 17°N) and Mexico (north of 17°N), respectively, from 1948 to 2015. The area-averaged winter precipitation in Central America exhibits larger interannual variability than in Mexico, with the corresponding standard deviations of 0.40 and 0.24 mm day^{-1}, respectively. The correlation coefficient between the two time series is −0.02, indicating that the overall variations of winter precipitation over Central America and Mexico are largely independent. Additionally, a trend of decreasing precipitation (−0.05 mm day^{-1} per decade) is found over Central America, whereas virtually no trend (0.005 mm day^{-1} per decade) is found for Mexico. It is also evident that the precipitation anomalies averaged over the two regions have been largely negative since 2000, consistent with the prolonged droughts in CAM.

3.2 Covariability between CAM precipitation and tropical SST

To quantify the relationship between CAM precipitation and tropical SST, an SVD analysis is performed based on the covariance matrices of winter season CAM precipitation and SSTs in the tropical Pacific and Atlantic basins (30°S–30°N, 120°E–30°E). Table 1 summarizes the statistics of two leading SVD modes, including the percentage of covariance explained by each mode, the temporal correlation coefficient between each pair of the SVD time

Table 1 Statistics of two leading SVD modes of winter (JFM) tropical Pacific/Atlantic SST and MCA precipitation (Pr) based on 1948–2015 observational data, including the percentage of covariance explained by each mode, the temporal correlation between pairs of SVD time series, and the variance of individual fields explained by each mode

SVD mode	Covariance (%)	Correlation	SST variance (%)	Pr variance (%)
Mode 1	67	0.70	37	17
Mode 2	20	0.63	15	15

series, and the percentage of variance in individual fields explained by each mode. Together the two modes account for 87% of the covariance between the SST and precipitation fields, and the corresponding components account for 52% of the SST variance and 32% of the precipitation variance, respectively. The spatial patterns of the two leading SVD modes are shown in Fig. 2 in the form of homogeneous correlation maps (Wallace et al. 1992) for both SST and precipitation.

The first SVD mode of SST (Fig. 2a) displays a typical La Niña SST pattern, with large negative correlations in the eastern and central tropical Pacific and positive correlations in the western tropical Pacific. Additionally, there are negative and positive correlations along the west coast of North America and in the central North Pacific, respectively. Associated with La Niña, negative SST anomalies are also found across the tropical Atlantic and Indian Ocean, consistent with the interactions between ENSO and the tropical Atlantic/Indian Ocean documented in previous studies (e.g., Wang et al. 2013; Zhu and Shukla 2013; Zhu et al. 2015; Terray et al. 2016). This mode explains 37% of the total tropical Pacific and Atlantic SST variance (Table 1). The precipitation component of the first SVD mode accounts for 17% of the total CAM winter precipitation variance (Table 1). The precipitation pattern (Fig. 2b) shows large negative correlations in northern and central Mexico and positive correlations in Central America. Therefore, associated with La Niña, winter tends to be drier than normal in Mexico, but wetter than normal in Central America, consistent with previous studies (Cavazos and Hastenrath 1990; Magana et al. 2003; Seager et al. 2009).

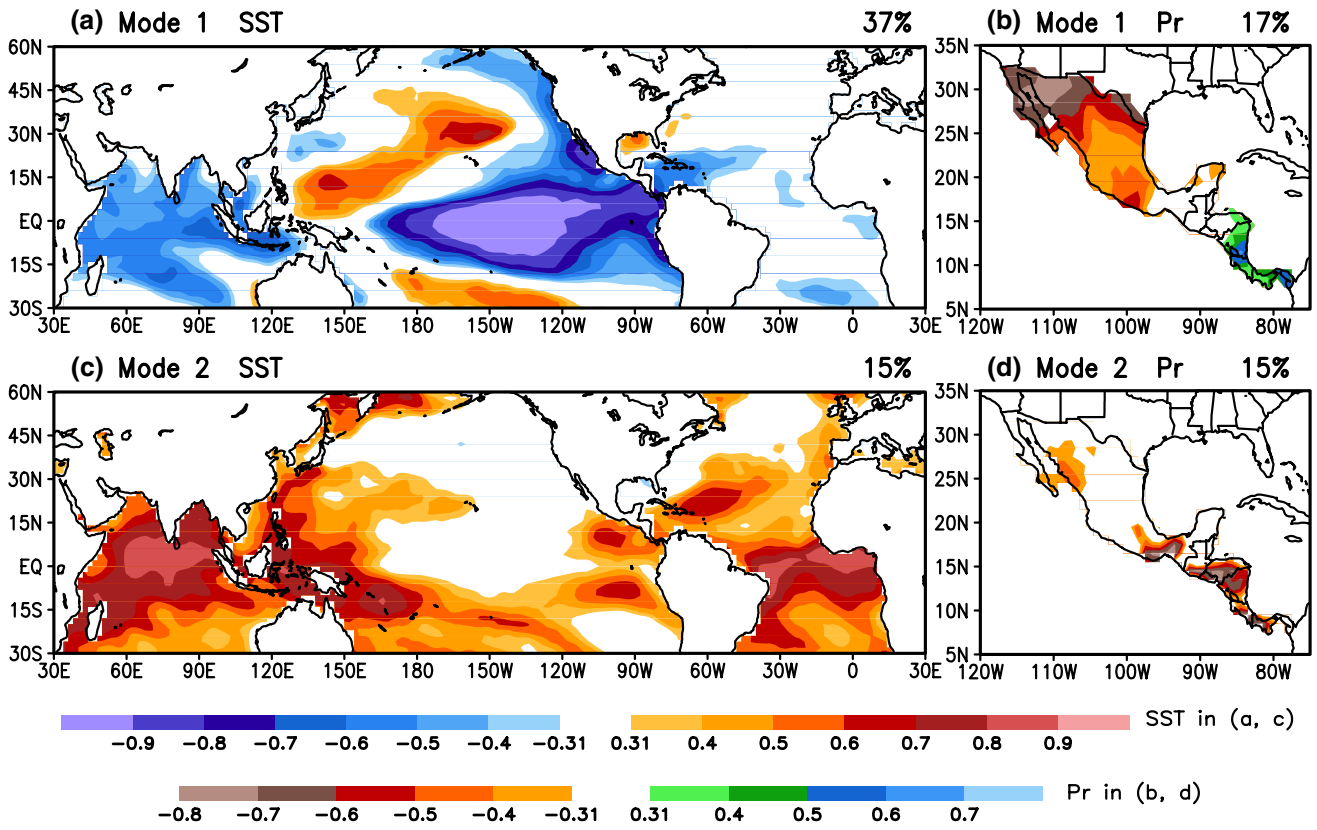

Fig. 2 Homogeneous correlation maps of the first (*top panels*) and second (*bottom panels*) SVD modes between **a, c** winter SST in the tropical Pacific and Atlantic and **b, d** precipitation in Mexico/Central America based on observations from 1948 to 2015. The correlations shown in *shadings* (>0.31 or <–0.31) are above the 99% significance level. The percentage of the total variance explained by each mode for SST (*left panels*) and precipitation (*right panels*) is listed at the *top right of each panel*

The second SVD mode of SST is characterized by two broad regions of positive correlations spanning across the tropical Atlantic basin and the tropical Indian Ocean–western Pacific sector (Fig. 2c). The precipitation in the second mode has a spatially coherent pattern with large negative correlations in Central America and southern Mexico (Fig. 2d), the region with large mean winter precipitation (Fig. 1a). The second mode thus represents a link between a general warming in the tropical oceans and winter drought in Central America and southern Mexico. This mode accounts for 15% of the SST variance, much less than the first mode (37%). However, it also accounts for 15% of the precipitation variance, which is comparable to mode 1 precipitation (17%).

The two pairs of the SVD time series of SST and precipitation are show in Fig. 3. The temporal correlation between the SST and precipitation time series in mode 1 (Fig. 3a) is 0.70, well above the 99% significance level. The SST time series (red bars) exhibits large positive and negative values greater than one standard deviation in La Niña (1950, 1951, 1955, 1956, 1971, 1974, 1976, 1989, 1999, 2000, 2008, and 2011) and El Niño (1958, 1969, 1973, 1983, 1987, 1992, 1993, 1995, 1998, and 2010) years, respectively. The mode 1 precipitation time series (green bars) also show coherent positive (negative) fluctuations with La Niña (El Niño).

The time series of the negative of the Niño-3.4 SST index is also plotted in Fig. 3a (red open triangles). Both the SVD SST time series and the Niño-3.4 SST index display consistent interannual variations with a correlation coefficient of 0.98 between the two. In addition, the negative of precipitation anomalies averaged over Mexico (thick blue line in Fig. 1c) is also plotted in Fig. 3a (green open triangles). The area-averaged precipitation anomalies are highly correlated with the SVD mode 1 precipitation time series (0.81). Out of 68 years, in 57 years (84% of the entire period) the two precipitation time series have the same sign. The first SVD mode thus suggests a close relationship between cold (warm) phase of ENSO and dry (wet) conditions in Mexico and wet (dry) conditions in Central America. This mode explains 67% of the covariance between the SST and precipitation fields (Table 1), indicating the predominant role played by ENSO in the covariability between winter tropical SST and CAM precipitation.

The correlation between the SST and precipitation time series for the second SVD mode (Fig. 3b) is 0.63, also well above the 99% significance level. This mode explains 20%

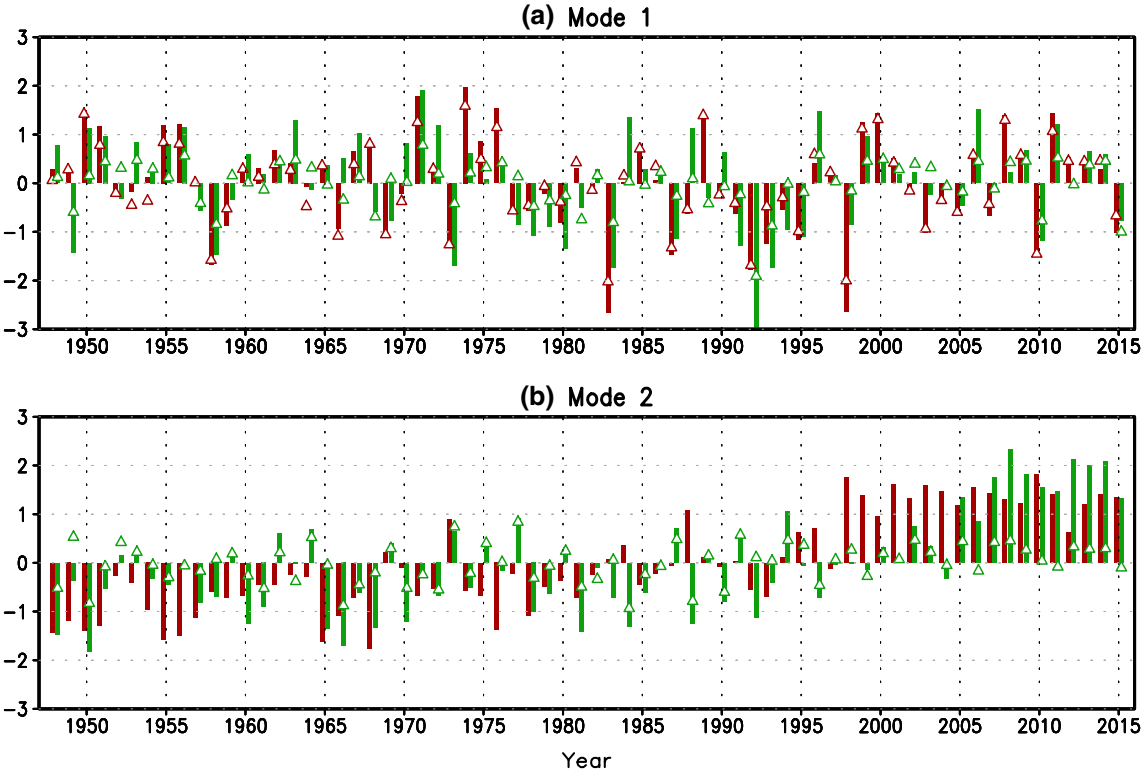

Fig. 3 Normalized SVD time series of winter (JFM) SST (*red bars*) and precipitation (*green bars*) from 1948 to 2015 for **a** the first and **b** the second modes. *Red open triangles* in **a** are the negative of the Niño-3.4 SST index (°C). *Green open triangles* in **a** are the negative of precipitation anomalies (mm day^{-1}) averaged over Mexico north of 17°N (*thick blue line* in Fig. 1c), which are multiplied by 2 for illustration purpose, and those in **b** are the negative of precipitation anomalies (mm day^{-1}) averaged over Central America south of 17°N (*thick red line* in Fig. 1c)

of the covariance between the two fields (Table 1). Both time series are characterized by an upward trend, with a transition of SST from cold anomalies to warm anomalies in the 1980s and 1990s. The timing of this change coincides with unprecedented warming of the global mean temperature in the late twentieth century (IPCC 2007). Associated with the SST warming trend, the mode 2 precipitation time series has persistent large positive values in the most recent decade (2005–2015). Superimposed on the mode 2 precipitation time series (green bars) are the precipitation anomalies averaged over Central America (green open triangles, also thick red line in Fig. 1c). The correlation between the two precipitation time series is 0.70 with 81% of the years (55 out of 68) having the same sign anomalies. The second SVD mode thus links the prolonged drought in Central America to the warming of tropical SST.

The SVD analysis confirms the relationship between wintertime CAM precipitation and tropical Pacific ENSO SST that has been documented in many previous studies. It also links an increase in the intensity of droughts in the CAM region during the last 20 years to the warming of SSTs in the tropical Atlantic, western Pacific, and Indian Ocean. Furthermore, the analysis quantifies these relationships and their relative importance to the variability of CAM winter precipitation (Table 1).

3.3 Associated atmospheric circulation

To understand the physical processes linking CAM precipitation to the tropical SST, Fig. 4 shows the circulation anomalies of 500-hPa height, 850-hPa wind, and 925-hPa divergence associated with the SVD mode 1 and mode 2 SSTs obtained based on linear regressions of 68-year data against the corresponding SVD SST time series. The 500-hPa height anomalies related to the mode 1 SST exhibit a typical Pacific/North American (PNA) pattern (Fig. 4a). The teleconnection pattern is characterized by an anomalous high over the North Pacific, a low over Canada, and another high over southern US and northern Mexico, indicating a wave train originating from the tropical Pacific in response to La Niña. As part of the wave train over the CAM region, the positive height anomalies to the north and negative anomalies to the south (Fig. 4c), respectively with low-level divergent and convergent flows, are dynamically consistent with the precipitation distribution in Fig. 2b. In addition, associated with La Niña, there is a strong easterly Caribbean low-level jet (Wang 2007), which enhances precipitation in Central America.

Associated with the mode 2 SST, the 500-hPa height field is dominated by positive anomalies in the tropics (Fig. 4b), consistent with the general warming of tropical SST (Fig. 2c). A wave train is also found over the PNA region, though the amplitude of anomalies is smaller than that in Fig. 4a. There are positive height anomalies downstream over the CAM region (Fig. 4d), which favor local dry conditions and are likely driven by warm SST anomalies in the adjacent oceans (Fig. 2c). Additionally, two centers of 925-hPa divergence (Fig. 4d) coincide with the precipitation deficits in Fig. 2d. The 850-hPa northwesterly wind anomalies in the Caribbean Sea suppress local low-level jet, conducive for less precipitation in Central America. The consistency between the circulation anomalies associated with SST and the precipitation anomalies in CAM suggests that the atmospheric circulation links the variations between tropical SST and CAM precipitation depicted by the two SVD modes.

3.4 Relationship between CAM precipitation and tropical SST in AMIP simulations

To ascertain whether the precipitation anomalies identified in the observational analysis (Fig. 2b, d) are the responses to the tropical SSTs (Fig. 2a, c), the SVD analysis is also applied to the 18-member ensemble mean CAM precipitation of the AMIP simulations and the SST in the tropical Atlantic and Pacific. The latter was prescribed as a boundary forcing to drive the model. Therefore, any signals of the ensemble mean precipitation may indicate the precipitation response to the SST.

Figure 5 shows the spatial distribution of the homogeneous correlations (Wallace et al. 1992) of the three leading SVD modes for both the wintertime SST and precipitation fields. The first SVD mode (Fig. 5a, b) displays similar SST and precipitation patterns to the observations (Fig. 2a, b), suggesting the out-of-phase precipitation anomalies in Central America and Mexico are the response to the ENSO SST. Unlike the second mode of SST in the observations (Fig. 2c), the observed positive correlations in the western Pacific and South Pacific convergence zone show up in the second mode of the AMIP simulations (Fig. 5c), whereas the observed positive correlations in the Indian Ocean and tropical Atlantic (Fig. 2c) appear in the third mode of the AMIP simulations (Fig. 5e). In response to the second and third modes of tropical SSTs (Fig. 5c, e), negative correlations are found in the precipitation field over the southern and central Mexico (Fig. 5d) and Central America (Fig. 5f), respectively, which are consistent with the second SVD mode of precipitation in Fig. 2d. The counterpart of the second mode in observations thus spreads into the second and third modes in the AMIP simulations.

The time series of the three SVD modes are shown in Fig. 6. Both the SST (red bars) and model precipitation (green bars) exhibit strong interannual variability in the first mode (Fig. 6a) and an upward trend in the second and third modes. The correlation between the two SST time series of the first mode (red bars, Figs. 3a, 6a) is 0.99 over the common period of 1957–2015, indicating that the ENSO-related

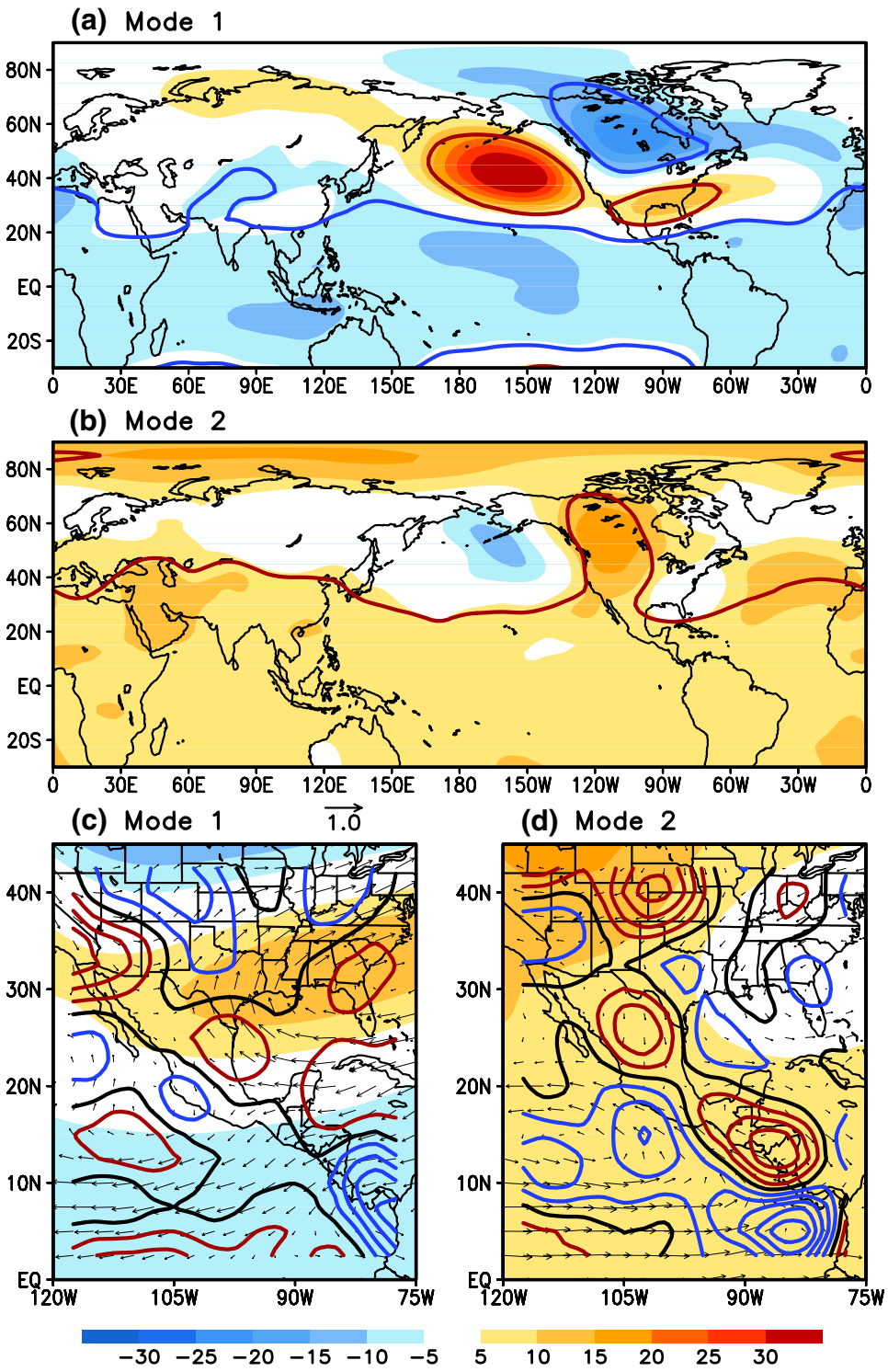

Fig. 4 Circulation anomalies of **a, b** 500-hPa height (gpm), **c, d** 850-hPa wind (vector, m s^{-1}) and 925-hPa divergence (contour, s^{-1}) associated with one standard deviation of the SVD SST time series, obtained based on linear regressions against the SVD SST time series for mode 1 (**a, c**) and mode 2 (**b, d**) using observational data. Contour interval in **c, d** is 2.0×10^{-7} s^{-1}, with positive in *red*, negative in *blue*, and zero contour in *thick black*. *Shadings* in **c, d** are same as in **a, b**. The height anomalies circled by *red* (*blue*) *lines* in **a, b** are positively (negatively) correlated with the SVD SST trim series above the 99% significance level

mode in the observations is well picked out in the AMIP simulations. The correlations of the SST time series of the second mode in the observations (red bars, Fig. 3b) with those of the second and third modes in the AMIP simulations (red bars, Fig. 6b, c) are 0.56 and 0.42, respectively, both exceeding the 99% significance level (0.33). The model results (Figs. 5c–f, 6b, c) suggest that the prolonged droughts in CAM in recent decades (Figs. 2d, 3b) are indeed the responses to the warming of SST in the tropical Atlantic, western Pacific, and Indian Ocean.

Table 2 summaries the statistics of the three SVD modes. Together the three modes count for 96% of covariance between the SST and precipitation fields, higher than

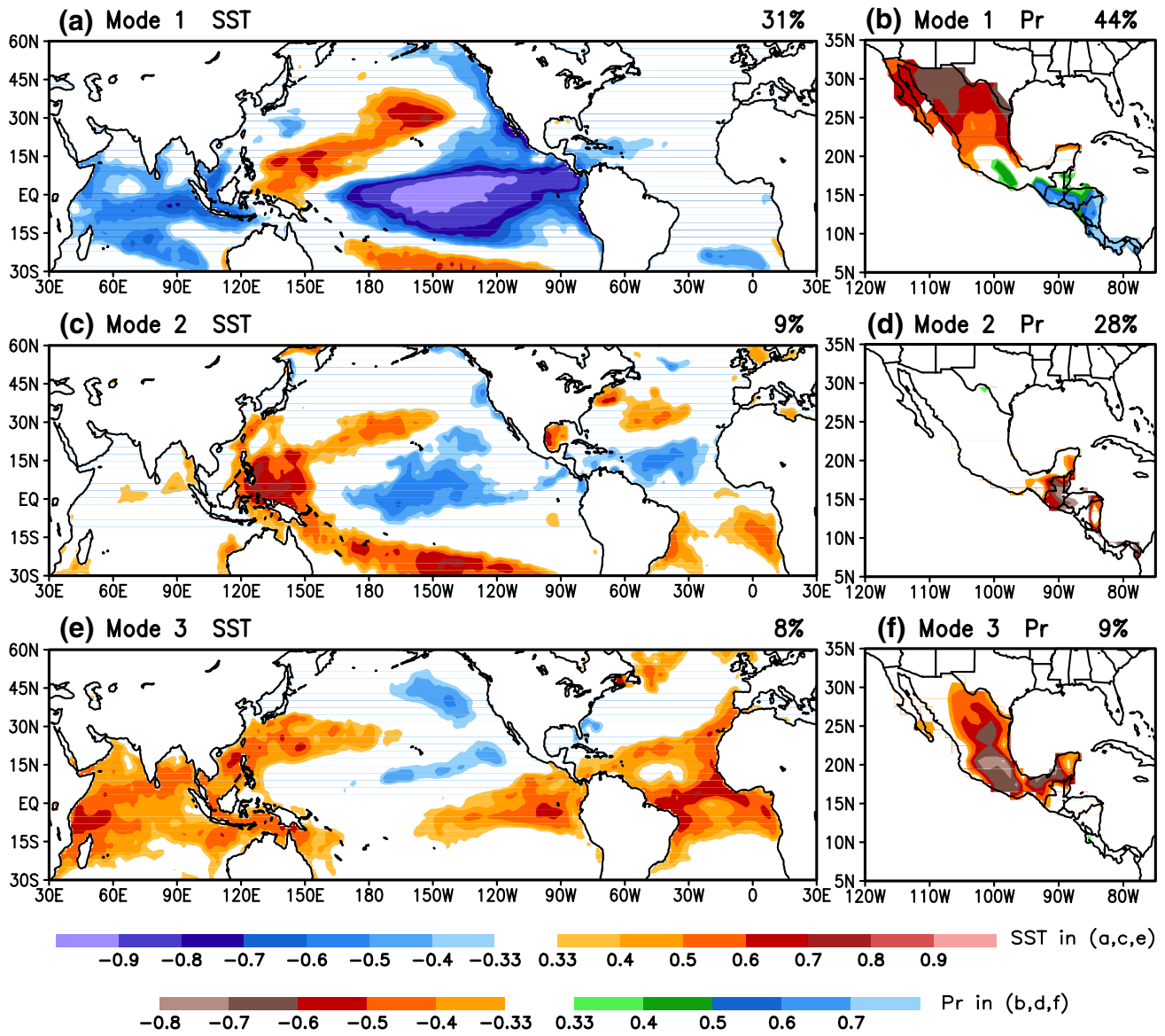

Fig. 5 Same as Fig. 2, but for the three leading SVD modes based on 18-member ensemble mean AMIP simulations from 1957 to 2015. The correlations shown in *shadings* (>0.33 or <–0.33) are above the 99% significance level

the two leading modes in the observations (87%, Table 1). Similar to the observations, the correlation between each pair of the SVD time series is highly significant, ranging from 0.61 to 0.73. The total SST variance represented by the three modes is 48%, comparable to the observations (52%). However, the precipitation variance explained by the three modes in the model is much higher than that in the observations (81 vs. 32%). The higher percentages of the covariance between the two fields and the precipitation variance explained are due to the ensemble average procedure, which reduces the internal variability and thus amplifies the signal to noise ratio (Kumar and Hoerling 1995).

3.5 Potential predictability of CAM winter precipitation

The observational analysis presented in Figs. 2, 3 and 4 suggests that the variability of CAM winter precipitation is strongly tied to tropical Atlantic and Pacific SSTs through the atmospheric circulation. The AMIP simulations further confirm that the CAM precipitation associated with the tropical SSTs are the responses to the SST forcing. The tropical SSTs, thus, have potentially predictive value for the CAM winter precipitation. Given tropical Atlantic and Pacific SST patterns, for example, from operational seasonal climate forecast, the CAM precipitation can be predicted based on the relationship depicted by the SVD

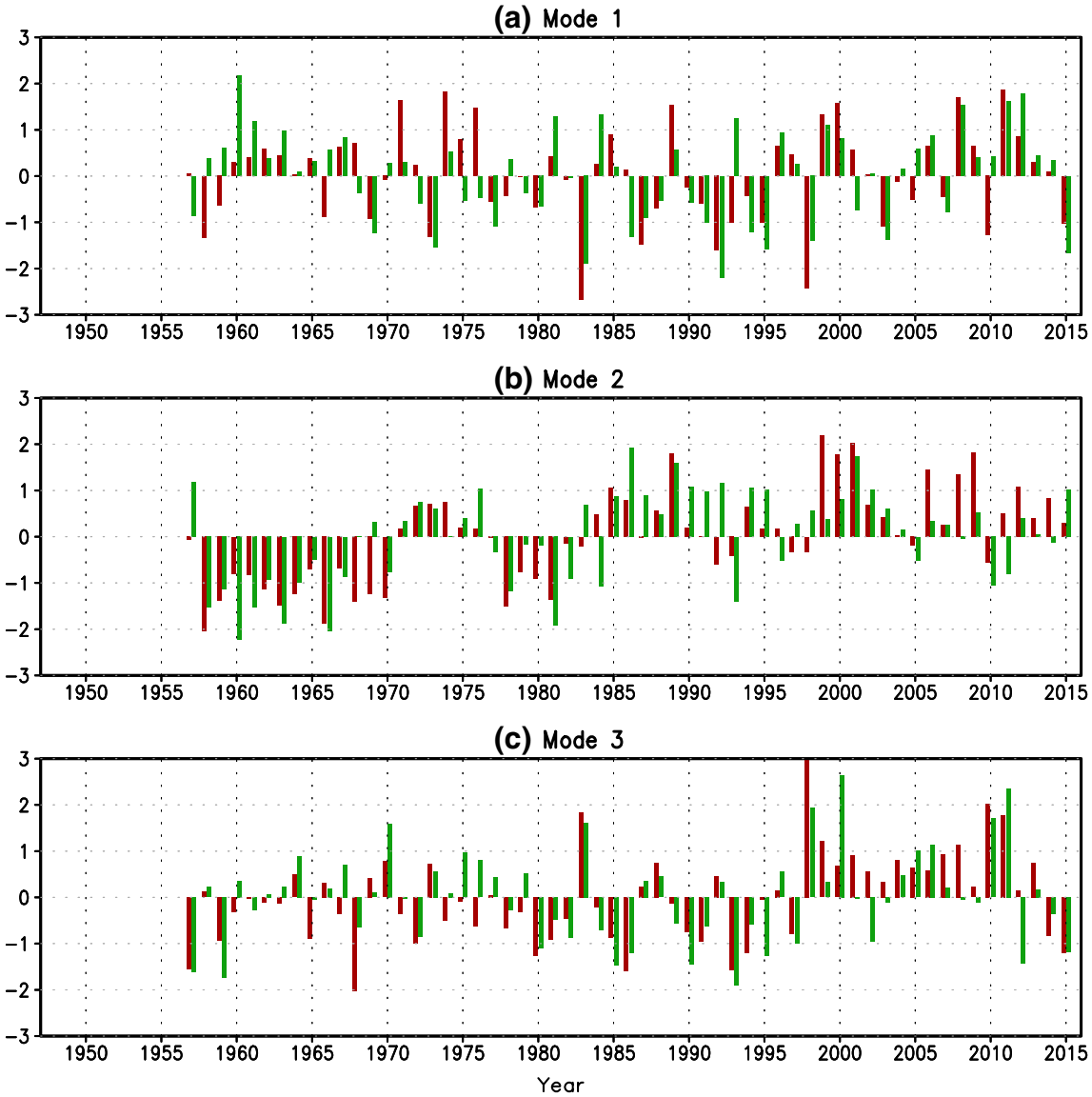

Fig. 6 Normalized SVD time series of winter (JFM) SST (*red bars*) and precipitation (*green bars*) for **a** the first, **b** the second, and **c** the third modes from the 18-member ensemble mean data of the 1957–2015 AMIP simulations

Table 2 Same as Table 1, but for the three leading SVD modes of winter (JFM) tropical Pacific/Atlantic SST and MCA precipitation (Pr) based on 18-member ensemble mean JFM data of the 1957–2015 AMIP simulations

SVD mode	Covariance (%)	Correlation	SST variance (%)	Pr variance (%)
Mode 1	73	0.61	31	44
Mode 2	17	0.66	9	28
Mode 3	6	0.73	8	9

analysis. The proposed forecast method can be similar to Wang et al. (1999) for the predictions of US precipitation.

The potential predictability of CAM winter precipitation can be assessed by (a) reconstructing precipitation anomalies based on the SVD SST time series with the target year removed from the training period, assuming that a coupled global climate model can accurately predict global SST, and (b) comparing the reconstructed precipitation with observations. First, a regression coefficient is obtained by regressing the observed JFM precipitation against the SVD SST time series for each grid point in CAM. A time series of precipitation is then constructed by the regression coefficient multiplied by the value of the SVD SST time series for each year.

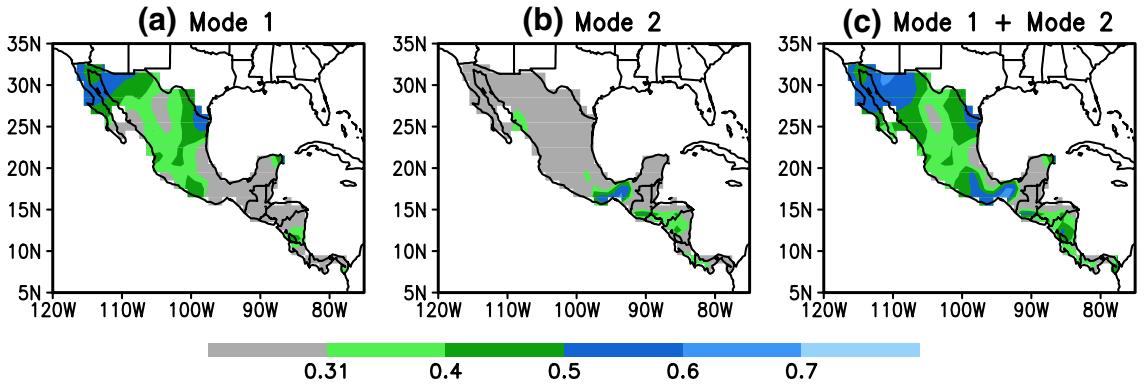

Fig. 7 Anomaly correlation between observed 1948–2015 JFM precipitation and reconstructed precipitation anomalies based on **a** SVD mode 1 SST time series, **b** SVD mode 2 SST time series, and **c** both mode 1 and mode 2 SST time series. *Color* (*grey*) *shadings* denote the correlations greater (smaller) than 0.31, which are above (below) the 99% significance level

Figure 7 shows the anomaly correlation between the observed precipitation and the constructed precipitation in CAM based on the first two individual SVD SST time series, as well as the two modes together. Considerable potential predictability is found in northern Mexico associated with the tropical Pacific SST (SVD mode 1, Fig. 7a) and in southern Mexico and Central America associated with the tropical Atlantic SST (SVD mode 2, Fig. 7b). When combining the two modes together (Fig. 7c), the anomaly correlations are above the 99% significance level over 75% of the CAM region. The results thus suggest significant potential predictability of CAM winter precipitation using the tropical SST information.

4 Summary and discussion

The covariability between CAM winter precipitation and tropical SST was objectively identified by the SVD analysis. Both tropical Pacific and Atlantic SSTs show a connection with the CAM precipitation variability. The first SVD mode captures the ENSO-related precipitation and ties droughts in northern Mexico to La Niña SST. The second mode connects droughts in Central America to the warming of the tropical Atlantic SST, as well as the warming in the tropical western Pacific and the tropical Indian Ocean. Each SVD precipitation pattern is consistent with the 500-hPa atmospheric circulation and low-level wind anomalies associated with the SVD SST, indicating the atmospheric bridge linking CAM precipitation and tropical SST. The SVD analysis shows 17% of CAM precipitation variance is related to the Pacific SST and 15% related to the Atlantic SST, suggesting that both are equally important in modulating CAM winter precipitation. The SVD analysis indicates that droughts in Central America in recent decades are related to the persistent warming of SST in the tropical Atlantic, western Pacific, and Indian Ocean. The AMIP simulations driven by the observed SST confirm that these precipitation anomalies in the CAM region are the responses to the tropical SST at the interannual and longer time scales. Therefore, tropical SSTs provide a source of predictability for CAM winter precipitation. Given a distribution of tropical SSTs, CAM winter precipitation may be predicted based on its relation to the SST identified by the SVD analysis.

The present work complements the previous studies on the relationships between CAM precipitation and SSTs in the adjacent tropical oceans (e.g., Enfield 1996; Enfield and Alfaro 1999; Taylor et al. 2002) in two aspects. First, the contributions of the tropical Pacific (17%) and Atlantic (15%) to the CAM winter precipitation are objectively quantified by the SVD analysis. Spatially, however, both show distinctive regional influence. The tropical Pacific SST has a broad influence across the CAM region (Fig. 2b). In contrast, the influence of tropical Atlantic SST is confined more to the south (Fig. 2d), where winter precipitation displays large mean values, as well as high interannual variability (Fig. 1a, b).

Second, the influence of the tropical Atlantic SST on the CAM precipitation projects more on the warming trend, rather than the interannual variability of the Atlantic SST found in the early observational studies (e.g., Enfield 1996; Enfield and Alfaro 1999; Taylor et al. 2002). With the continuous warming in the tropical Atlantic in the twenty-first century (Figs. 2c, 3b), it is reasonable to expect that the influence of the warming trend in the Atlantic SST may become predominant over the influence of the interannual SST variability on the CAM precipitation. With the additional impact of the interannual variability of Atlantic SST that has been identified in the previous studies, the tropical Atlantic could be more influential than the tropical Pacific in modulating CAM winter precipitation.

Recent modeling studies of climate projections (e.g., Karmalkar et al. 2011; Rauscher et al. 2011; Fuentes-Franco et al. 2015) based on the Coupled Model Intercomparison Project (CMIP) simulations (Meehl et al. 2007; Taylor 2012) have shown that under a future warmer climate, the warming of the tropical Atlantic could significantly reduce precipitation in CAM. The results in this study indicate that the impact of global warming on the CAM precipitation detected in the future climate projections is also found in the observational record.

As CAM is characterized by monsoon precipitation which peaks in summer, applying the same methodology to warm season CAM precipitation will be a logical extension of this work. Additionally, both changes in the ENSO characteristics and intense warming of tropical oceans are projected to occur in the coming decades (e.g., Stevenson 2012). How these could affect CAM precipitation variability, and its relation to the adjacent oceans in the future is also an interesting topic. Through a comparison of multi-model simulations for the present-day climate and future projections, like Mariotti et al. (2015) did for the Mediterranean region using the CMIP simulations, the contribution of ENSO and global warming to CAM precipitation will be assessed in a subsequent study.

Acknowledgements The authors would like to thank two anonymous reviewers and the editor for their insightful and constructive comments and suggestions.

References

Bhattacharya T, Chiang JCH (2014) Spatial variability and mechanism underlying El Niño-induced droughts in Mexico. Clim Dyn 43:3309–3326

Bretherton CS, Smith C, Wallace JM (1992) An intercomparison of methods for finding coupled patterns in climate data. J Clim 5:541–560

Cavazos T, Hastenrath S (1990) Convection and rainfall over Mexico and their modulation by the southern oscillation. Int J Climatol 10:377–386

Chen M, Kumar A (2016) The utility of seasonal hindcast database for the analysis of climate variability: an example. Clim Dyn. doi:10.1007/s00382-016-3073-z

Chen M, Xie P, Janowiak JE, Arkin PA (2002) Global land precipitation: a 50-year monthly analysis based on gauge observations. J Hydrometeor 3:249–266

Enfield DB (1996) Relationship of inter-American rainfall to tropical Atlantic and Pacific SST variability. Geophys Res Lett 23:3305–3308

Enfield DB, Alfaro EJ (1999) The dependence of Caribbean rainfall on the interaction of the tropical Atlantic and Pacific Oceans. J Clim 12:2093–2103

Fuentes-Franco R, Coppola E, Giorgi F, Pavia EG, Diro GT, Graef F (2015) Inter-annual variability of precipitation over southern Mexico and Central America and its relationship to sea surface temperature from a set of future projections from CMIP5 GCMs and RegCM4 CORDEX simulations. Clim Dyn 45:425–440

Giannini A, Kushnir Y, Cane MA (2000) Interannual variability of Caribbean rainfall, ENSO, and the Atlantic ocean. J Clim 13:297–311

IPCC (2007) Climate change 2007: the physical science basis. In: Solomon S et al (ed) Contribution of Working Group I to the Third Assessment Report of the Intergovernmental Panel on Climate Change. Cambridge Univerity Press, Cambridge, p 996

Kalnay E et al (1996) The NCEP–NCAR 40-year reanalysis project. Bull Am Meteor Soc 77:437–471

Karmalkar AV, Bradley RS, Diaz HF (2011) Climate change in Central America and Mexico: regional climate model validation and climate change projections. Clim Dyn 37:605–629

Karnauskas KB, Busalacchi AJ (2009) The role of SST in the East Pacific warm pool in the interannual variability of Central American rainfall. J Clim 22:2605–2623

Kumar A, Hoerling MP (1995) Prospects and limitations of atmospheric GCM climate predictions. Bull Am Meteor Soc 76:335–345

Magaña VO, Vázquez JL, Pérez JL, Pérez JB (2003) Impact of El Niño on precipitation in Mexico. Geofisica Internacional 42:313–330

Mariotti A, Pan Y, Zeng N, Alessandri A (2015) Long-term climate change in the Mediterranean region in the midst of decadal variability. Clim Dyn 44:1437–1456

Meehl GA et al (2007) Global climate projections. Climate Change 2007: the physical science basis. In: Solomon S et al (eds) Cambridge Univerity Press, Cambridge, pp 747–846

Mendez M, Magana V (2010) Regional aspects of prolonged meteorological droughts over Mexico and Central America. J Clim 23:1175–1188

OCHA (2014) Drought in Central America, Situation Report No. 1 (December 10, 2014), the United Nations' Region Office for Latin America and the Caribbean

Pavia EG, Graef F, Reyes J (2006) PDO–ENSO effects in the climate of Mexico. J Clim 19:6433–6438

Peng P, Kumar A (2005) A large ensemble analysis of the influence of tropical SSTs on seasonal atmospheric variability. J Clim 18:1068–1085

Rauscher SA, Kucharski F, Enfield DB (2011) The role of regional SST warming variations in the drying of Meso-America in future climate projections. J Clim 24:2003–2016

Rayner NA, Parker DE, Horton EB, Folland CK, Alexander LV, Rowell DP, Kent EC, Kaplan A (2003) Global analysis of sea surface temperature, sea ice, and night marine air temperature since the late nineteenth century. J Geophys Res 108:4407

Reynolds RW, Rayner NA, Smith TM, Stokes DC, Wang W (2002) An improved in situ and satellite SST analysis for climate. J Clim 15:1609–1625

Rodriguez OR (2012) North Mexico drought worst on record. *Huffington Post*

Saha S et al (2014) The NCEP climate forecast system version 2. J Clim 27:2185–2208

Seager R, Ting M, Davis M, Cane M, Naik N, Nakamura J, Li C, Cook E, Stahle DW (2009) Mexican drought: an observational modeling and tree ring study of variability and climate change. Atmosfera 22:1–31

Smith TM, Reynolds RW, Peterson TC, Lawrimore J (2008) Improvements to NOAA's historical merged land–ocean surface temperature analysis (1880–2006). J Clim 21:2283–2296

Snedecor GW, Cochran WG (1989) Statistical Methods, 8th edn. Iowa State Univ. Press, p 503

Stevenson SL (2012) Significant changes to ENSO strength and impacts in the twenty-first century: results from CMIP5. Geophys Res Lett 39:L17703

Taylor MA, Enfield DB, Chen AA (2002) Influence of the tropical Atlantic versus the tropical Pacific on Caribbean rainfall. J Geophys Res 107:3127

Taylor KE, Stouffer RJ, Meehl GA (2012) An overview of CMIP5 and the experiment design. Bull Am Meteor Soc 93:485–498

Terray P, Masson S, Prodhomme C, Roxy MK, Sooraj KP (2016) Impacts of Indian and Atlantic oceans on ENSO in a comprehensive modeling framework. Clim Dyn 46:2507–2533

Ting M, Wang H (1997) Summertime United States precipitation variability and its relation to Pacific sea surface temperature. J Clim 10:1853–1873

Wallace JM, Smith C, Bretherton CS (1992) Singular value decomposition of wintertime sea surface temperature and 500-mb height anomalies. J Clim 5:561–576

Wang C (2007) Variability of the Caribbean low-level jet and its relations to climate. Clim Dyn 29:411–422

Wang H, Fu R (2000) Winter monthly mean atmospheric anomalies over the North Pacific and North America associated with El Niño SSTs. J Clim 13:3435–3447

Wang H, Kumar A (2015) Assessing the impact of ENSO on drought in the US Southwest with the NCEP climate model simulations. J Hydrol 526:30–41

Wang H, Ting M (2000) Covariabilities of winter US precipitation and Pacific sea surface temperature. J Clim 13:3711–3719

Wang H, Ting M, Ji M (1999) Prediction of seasonal mean United States precipitation based on El Nino sea surface temperatures. Geophys Res Lett 26:1341–1344

Wang H, Fu R, Kumar A, Li W (2010) Intensification of summer rainfall variability in the southern United States during recent decades. J Hydrometeor 11:1007–1018

Wang H, Kumar A, Wang W, Jha B (2012) US summer precipitation and temperature patterns following the peak phase of El Niño. J Clim 25:7204–7215

Wang H, Kumar A, Wang W (2013) Characteristics of subsurface ocean response to ENSO assessed from simulations with the NCEP Climate Forecast System. J Clim 26:8065–8083

Zhu J, Shukla J (2013) The role of air-sea coupling in seasonal prediction of Asia-Pacific summer monsoon rainfall. J Clim 26:5689–5697

Zhu J, Huang B, Kumar A, Kinter JL III (2015) Seasonality in prediction skill and predictable pattern of tropical Indian Ocean SST. J Clim 28:7962–7984